

Channeling quantum criticality

Yijian Zou,¹ Shengqi Sang,² and Timothy H. Hsieh²

¹Stanford Institute for Theoretical Physics, Stanford University, Stanford, CA 94305, USA

²Perimeter Institute for Theoretical Physics, Waterloo, Ontario N2L 2Y5, Canada

We analyze the effect of decoherence, modelled by local quantum channels, on quantum critical states and we find universal properties of the resulting mixed state's entanglement, both between system and environment and within the system. Renyi entropies exhibit volume law scaling with a subleading constant governed by a “ g -function” in conformal field theory (CFT), allowing us to define a notion of renormalization group (RG) flow (or “phase transitions”) between quantum channels. We also find that the entropy of a subsystem in the decohered state has a subleading logarithmic scaling with subsystem size, and we relate it to correlation functions of boundary condition changing operators in the CFT. Finally, we find that the subsystem entanglement negativity, a measure of quantum correlations within mixed states, can also exhibit log scaling. We illustrate these phenomena for the critical ground state of the transverse-field Ising model, in which we identify four RG fixed points of dephasing channels and verify the RG flow numerically. Our results are relevant to quantum critical states realized on noisy quantum simulators, in which our predicted entanglement scaling can be probed via shadow tomography methods.

Introduction – Quantum devices have advanced significantly to the point of challenging classical computers in sampling and simulation tasks [1–5]. In the context of quantum many-body physics, they are promising experimental platforms for realizing long-range entangled quantum phases of matter including topological order [6, 7] and quantum critical states [8]. Furthermore, their controllability at the single qubit level enables the exploration of quantum dynamics beyond simple time evolution with a Hamiltonian, and one prominent example is dynamics involving both unitary evolution and projective measurements [9–15]. Nevertheless, quantum devices are noisy and any states prepared are subject to decoherence. One important question is which properties of quantum matter survive in a noisy environment, and how to understand any residual order in the mixed state? Recently, substantial progress has been made in understanding mixed state versions of gapped quantum systems including symmetry protected topological phases and topological order [16–21].

In this work, we study quantum critical states under decoherence, modelled by local quantum channels. A point of inspiration is prior work [22–25] which found that measurements (with outcomes recorded) can have a significant effect on quantum critical states, in some cases boosting long range correlation. However, verifying such effects typically requires post-selecting on monitored pure state trajectories. In contrast, quantum channels can be viewed as environmental measurement in which the outcomes are averaged over, and we are interested in properties of the resulting mixed state, thus avoiding the need for post-selection.

Naively one might expect that local quantum channels generically have little qualitative effect since they can be represented as finite depth unitaries acting on an enlarged Hilbert space, and such finite depth unitaries cannot alter long-distance correlations. While this is true

for linear observables of the state, non-linear quantities like entanglement measures can be significantly affected by local channels.

Indeed, a key finding of our work is that for entanglement measures like Renyi entropies and entanglement negativity, local quantum channels acting on quantum critical states can drive phase transitions or more technically, renormalization group (RG) flows, between different conformal fixed points labeling different quantum channels. More specifically, we find that in computing such measures, quantum channels map to boundary conditions for multiple copies of the original conformal field theory (CFT) describing the critical state. Under coarse-graining, such boundary conditions can flow to a variety of conformal fixed points whose classification can be much richer than that of the single copy CFT.

Concretely, we find that the Renyi entropy of the decohered state, which quantifies the entanglement between system and environment, is extensive but has a subleading term dictated by a “ g -function” in CFT. This g -function characterizes the channel with respect to Renyi entropy and dictates the direction of RG flow between two channels: a channel with a larger g can flow to a channel with smaller g if weakly perturbed by the latter. Moreover, near a RG fixed point, the g -function has a universal scaling form determined by critical exponents.

We also find that the Renyi entropy of a subsystem A of the decohered state has a subleading logarithmic scaling with $|A|$ and its coefficient is given by scaling dimensions of certain boundary condition changing operators. Likewise, we find that the entanglement negativity between A and its complement, which quantifies quantum correlations within the system, can also exhibit log scaling with $|A|$. We demonstrate all these features for the one dimensional transverse field Ising critical point and explicitly illustrate the RG flow between different quantum channels. These universal aspects of entanglement

and entropy in channeled criticality can be probed in quantum simulators using shadow tomography methods [26, 27].

Quantum channels– We first review useful facts about quantum channels [28]. A quantum channel represents the most general quantum process including decoherence. Formally, it is a completely positive trace-preserving map $\rho \rightarrow \mathcal{N}(\rho)$ acting on density matrices. For a quantum channel, one may define its dual-channel \mathcal{N}^* , which is a linear map on operators satisfying $\text{Tr}(\rho \mathcal{N}^*(O)) = \text{Tr}(\mathcal{N}(\rho)O)$, $\forall O$. The relation between \mathcal{N} and \mathcal{N}^* is illustrated in Fig. 1(a).

Here we consider a spatially uncorrelated noise model defined on a qubit chain. The noise can be modeled as a product of single-qubit channels $\mathcal{N} = \otimes_{j=1}^L \mathcal{N}_j$ where each \mathcal{N}_j is a channel acting on the j^{th} -qubit.

One example we focus on is the dephasing channel $\mathcal{N}_j = \mathcal{D}_{p,\vec{v}}$, which represents an environment-qubit coupling along the $\sigma_{\vec{v}} := v_x \sigma_x + v_y \sigma_y + v_z \sigma_z$ direction. The action of $\mathcal{D}_{p,\vec{v}}$ on a density matrix is

$$\mathcal{D}_{p,\vec{v}}(\rho) = \left(1 - \frac{p}{2}\right) \rho + \frac{p}{2} \sigma_{\vec{v}} \rho \sigma_{\vec{v}}. \quad (1)$$

The channel is self-dual, i.e., $\mathcal{D}_{p,\vec{v}}^* = \mathcal{D}_{p,\vec{v}}$. The parameter $p \in [0, 1]$ controls the strength of the noise: when $p = 0$, $\mathcal{D}_{p,\vec{v}}$ is the identity channel and leaves states unchanged; while if $p = 1$, $\mathcal{D}_{p,\vec{v}}$ turns any quantum state into a classical ensemble.

General formalism mapping information-theoretic quantities to quantum quench problem– We consider a critical ground state $|\psi\rangle$ under decoherence of the above type, resulting in density matrix $\rho = \mathcal{N}(|\psi\rangle\langle\psi|)$. We study information-theoretic quantities including n^{th} -Renyi entropy and entanglement negativity, and we map these quantities to quantum quench problems in $\text{CFT}^{\otimes 2n}$, i.e. a $2n$ -copied CFT.

We start with the Renyi entropy of a subsystem A : $S_A^{(n)}(\rho) := \frac{1}{1-n} \log \text{Tr}(\rho_A^n)$, where $\rho_A = \text{Tr}_{\bar{A}} \rho$. This is a measure of both quantum and classical correlation between A and rest of the system \bar{A} together with the environment. It reduces to the von-Neumann entropy after taking the replica limit $n \rightarrow 1$. The partition function $Z_A^{(n)} := \text{Tr}(\rho_A^n)$ can be rewritten as:

$$Z_A^{(n)} = \text{Tr}(\rho^{\otimes n} \tau_{n,A}) = \text{Tr}(\mathcal{N}(|\psi\rangle\langle\psi|)^{\otimes n} \tau_{n,A}), \quad (2)$$

where $\tau_{n,A} = \prod_{j \in A} \tau_{n,j}$ forward permutes the replicas for sites in A , and acts as identity for sites in \bar{A} . Next, we use the dual channel to rewrite

$$Z_A^{(n)} = \text{Tr}(|\psi\rangle\langle\psi|^{\otimes n} B_{\mathcal{N},A}), \quad (3)$$

where $B_{\mathcal{N},A} := \mathcal{N}^{*\otimes n}(\tau_{n,A}) = \otimes_{j \in A} \mathcal{N}_j^{*\otimes n}(\tau_{n,j})$. The two ways to write the expression are graphically shown in Fig. 1(b). Finally, we use the standard folding trick for defect CFT [29] to treat each operator O as a state

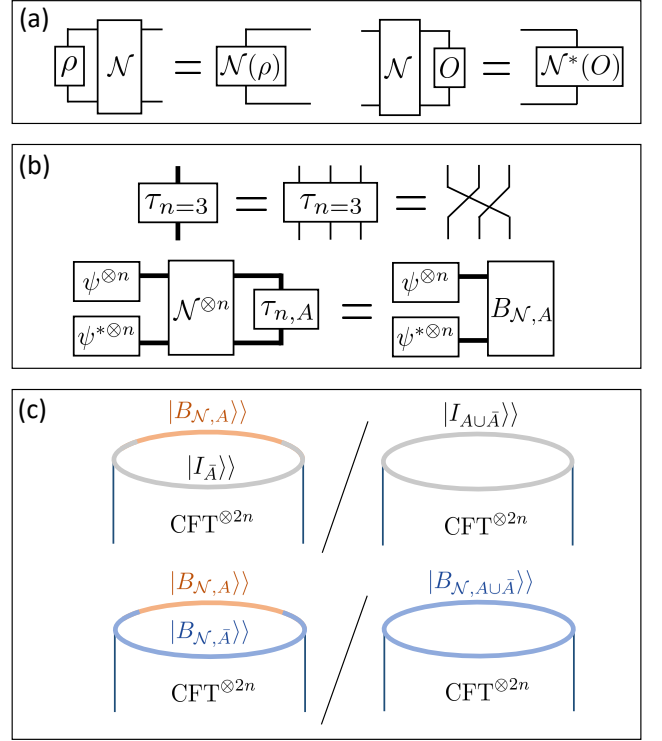


FIG. 1. (a) Diagrammatic representation of a quantum channel and its dual channel’s action. (b) Top: graphical representation of tensor τ_n ($n = 3$) that forward permutes replicas. Each thick leg represents a n -copied original Hilbert space. Bottom: The two expressions of $Z_A^{(n)}$ in Eqs. (2) and (3). (c) Top: path integral representation of Eq. (4), used for computing Renyi entropy. Note that the denominator is $\langle\psi^{\otimes n}|\psi^{\otimes n}\rangle = 1$. Bottom: path integral representation of the analogous object for Renyi negativity Eq. (5).

$|O\rangle\rangle$ in the doubled Hilbert space, whose inner product is defined as $\langle\langle O_1|O_2\rangle\rangle = \text{Tr}(O_1^\dagger O_2)$. Thus, under the folding,

$$Z_A^{(n)} = \langle\langle (\psi \otimes \psi^*)^{\otimes n} | B_{\mathcal{N},A} I_{\bar{A}} \rangle\rangle. \quad (4)$$

The bra-state $|\langle\langle (\psi \otimes \psi^*)^{\otimes n} \rangle\rangle$ is $2n$ copies of the critical state, while the ket-state $|B_{\mathcal{N}}\rangle\rangle$ is a product state, since the operator $B_{\mathcal{N},A}$ factorizes among j . Thus, we have reformulated the Renyi entropy as a quantum quench problem from a product state $|B_{\mathcal{N}}\rangle\rangle$ to a $2n$ -copied CFT, whose path integral representation on the space-time manifold is shown in Fig. 1(c, top).

The other quantity that we consider is n -th (n is odd) Renyi entanglement negativity $N_A^{(n)}(\rho) := \frac{1}{1-n} \log \frac{\text{Tr}(\{\rho^{TA}\}^n)}{\text{Tr}(\rho^n)}$ for a subsystem A , where $(\cdot)^{TA}$ is the partial-transpose operation that swaps the bra and ket states in ρ for sites within A . $N_A^{(n)}$ is a measure of quantum correlation between A and the rest of the system \bar{A}

[30, 31]. A similar derivation shows that

$$N_A^{(n)}(\rho) = \frac{1}{1-n} \log \frac{\langle\langle (\psi \otimes \psi^*)^{\otimes n} | B_{\mathcal{N},A} \tilde{B}_{\mathcal{N},\bar{A}} \rangle\rangle}{\langle\langle (\psi \otimes \psi^*)^{\otimes n} | B_{\mathcal{N},A \cup \bar{A}} \rangle\rangle}. \quad (5)$$

where $\tilde{B}_{\mathcal{N},\bar{A}} = \otimes_{j \in \bar{A}} \mathcal{N}_j^{*\otimes n}(\tau_{n,j}^{-1})$. Thus the calculation of $N_A^{(n)}$ is mapped to a quantum quench from another product initial state to the same $2n$ -copied CFT, see Fig. 1(c, bottom).

In such quantum quench problems, it has been shown [32–35] that a short-range correlated state can be described by a conformal boundary condition at long distances. We will assume that this is the case for product states $|B_{\mathcal{N}}\rangle\rangle$ and $|\tilde{B}_{\mathcal{N}}\rangle\rangle$ [36].

The g function– We now focus on the simplest quantity

$$S^{(n)}(\rho) = \frac{1}{1-n} \log Z^{(n)}(L), \quad (6)$$

where L is the total system size. This is the Renyi entropy of the whole system, or alternatively, the Renyi entanglement entropy between system and environment. In a boundary CFT, the partition function $Z^{(n)}(L)$ depends on UV details, but one can define a UV-independent g -function [37–39],

$$\log g^{(n)}(L) = \left(1 - L \frac{d}{dL}\right) \log Z^{(n)}(L). \quad (7)$$

which plays a similar role for boundary RG flow as the central charge c -function plays for bulk RG flow. It satisfies the following two properties. First, $\log g^{(n)}(L)$ is a monotonically decreasing function of L . Second, for conformal boundary conditions (RG fixed points), $\log g^{(n)}(L) = \log g^{(n)}$ is independent of L , which equals the universal Affleck-Ludwig boundary entropy [40]. At these fixed points, solving the differential equation (7) gives $\log Z^{(n)}(L) = (1-n)\alpha^{(n)}L + \log g^{(n)}$, where $(1-n)\alpha^{(n)}$ is a non-universal integration constant. One of our main results

$$S^{(n)}(\rho) = \alpha^{(n)}L - \frac{1}{n-1} \log g_{\mathcal{N}}^{(n)} \quad (8)$$

then follows from Eq. (6). Given a lattice wavefunction, we may compute $g_{\mathcal{N}}^{(n)}(L)$ numerically using Eq. (7). We identify a channel \mathcal{N} as a RG fixed point if $g_{\mathcal{N}}^{(n)}(L)$ becomes a constant $g_{\mathcal{N}}^{(n)}$ as L exceeds a few lattice spacings. The identity channel \mathcal{I} is always a RG fixed point with $\log g_{\mathcal{I}}^{(n)} = 0$.

RG flow near a fixed point– Let \mathcal{N}_p be a family of quantum channels parameterized by p (e.g, p in the dephasing channel $\mathcal{D}_{p,\bar{v}}$). We denote the g function of \mathcal{N}_p as $g_p^{(n)}(L)$. Let $p = p_c$ be a RG fixed point with the g -function g_c . Near $p = p_c$, the RG flow equation can be linearized: $\frac{dp}{d \log L} = (p - p_c)/\nu$, which implies $|p(L) - p_c| \sim L^{1/\nu}$ for

the effective $p(L)$ at length scale L . The g -function only depends on the latter, and thus

$$g_p^{(n)}(L) = \bar{g}^{(n)}(|p - p_c|L^{1/\nu}). \quad (9)$$

ν is the analog of the ‘‘correlation length exponent’’ in critical phenomena. If $\nu > 0$, then the fixed point \mathcal{N}_{p_c} is unstable, and it flows into another fixed point with the g -function $g' < g_c$. In such cases, the scaling function $\bar{g}^{(n)}$ is a monotonically decreasing function with $\bar{g}^{(n)}(0) = g_c$ and $\bar{g}^{(n)}(\infty) = g'$.

Subsystem entropy– Now we consider the entropy of a subsystem, whose corresponding quantum quench problem is from a spatially inhomogeneous initial state, see Fig. 1(c, top). Such initial state can be described in CFT by inserting boundary condition changing operator $\phi_{\mathcal{IN}}^{(n)}$ and $\phi_{\mathcal{NI}}^{(n)} = \phi_{\mathcal{IN}}^{(n)*}$ at the intersections [41–43]. There are $2m$ insertions if A contains m disjoint intervals. In particular, if A is a single interval with length L_A , then the partition function $Z^{(n)}(L)$ is

$$\langle\langle \phi_{\mathcal{IN}}^{(n)}(0) \phi_{\mathcal{IN}}^{(n)*}(L_A) \rangle\rangle = C \left(\frac{L}{\pi} \sin \frac{\pi L_A}{L} \right)^{-2\Delta_{\mathcal{IN}}^{(n)}}, \quad (10)$$

where $\Delta_{\mathcal{IN}}^{(n)}$ is the scaling dimension of $\phi_{\mathcal{IN}}^{(n)}$ and C is a normalization constant. Eq. (10) together with Eq. (6) gives another main result

$$S^{(n)}(\rho_A) = \alpha^{(n)}L_A + \frac{2\Delta_{\mathcal{IN}}^{(n)}}{n-1} \log \left(\frac{L}{\pi} \sin \left(\frac{\pi L_A}{L} \right) \right) + O(1). \quad (11)$$

In order to numerically verify the formula, it is useful to consider the Renyi mutual information $I^{(n)}(A, B) = S^{(n)}(\rho_A) + S^{(n)}(\rho_B) - S^{(n)}(\rho_{AB})$. Choosing $B = \bar{A}$ to be the complement of A , we obtain

$$I^{(n)}(A, \bar{A}) = \frac{4\Delta_{\mathcal{IN}}^{(n)}}{n-1} \log \left(\frac{L}{\pi} \sin \left(\frac{\pi L_A}{L} \right) \right) + O(1), \quad (12)$$

in which the volume law pieces have cancelled each other. Similar results hold for Renyi negativity $N_A^{(n)}(\rho)$, except that the boundary condition changing operator is different.

For two disjoint intervals $A = [x_1, x_2], B = [x_3, x_4]$, we can show that $I^{(n)}(A, B)$ is only a function of the cross ratio $\eta = (X_{12}X_{34})/(X_{13}X_{24})$, where $X_{ij} = \sin(\pi|x_i - x_j|/L)$. At small η , we may fuse the two boundary condition changing operators $\phi_{\mathcal{IN}}^{(n)} \times \phi_{\mathcal{IN}}^{(n)*} = I + O^{(n)} + \dots$, where $O^{(n)}$ is the second lowest operator in the operator product expansion. This implies the scaling

$$I^{(n)}(A, B) = \text{const.} \times \eta^{\Delta_O^{(n)}} \quad (\eta \ll 1). \quad (13)$$

Note that $O^{(n)}$ is a boundary operator at the boundary condition $|S_{\mathcal{I}}\rangle\rangle$, which we may unfold to get a bulk local operator in the n -copied CFT. Thus, $\Delta_O^{(n)}$ must be a sum of n scaling dimensions in the original CFT.

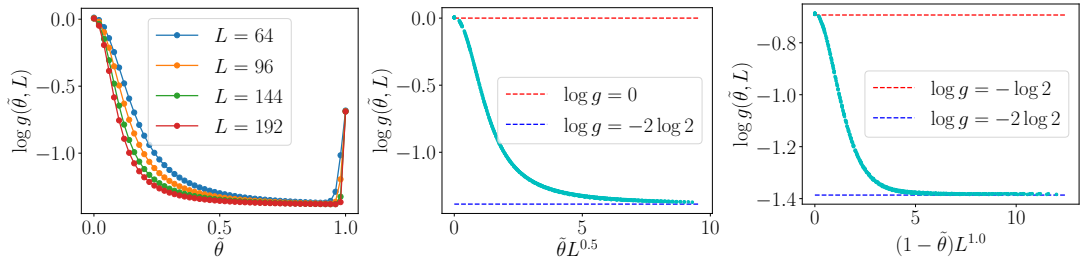


FIG. 2. g -function (universal subleading constant of Renyi entropy) for complete dephasing channel $\mathcal{D}_{p=1, \vec{v}}$ applied to critical Ising ground state, where $\vec{v} = (\sin(\pi\tilde{\theta}/2), 0, \cos(\pi\tilde{\theta}/2))$ in the XZ plane. Left: $g(\tilde{\theta}, L)$ for different L . Center: Data collapse for $0 \leq \tilde{\theta} \leq 0.6$, indicating RG flow from \mathcal{D}_z to \mathcal{D}_{zx} . Right: Data collapse for $0.95 \leq \tilde{\theta} \leq 1$, indicating RG flow from \mathcal{D}_x to \mathcal{D}_{zx} .

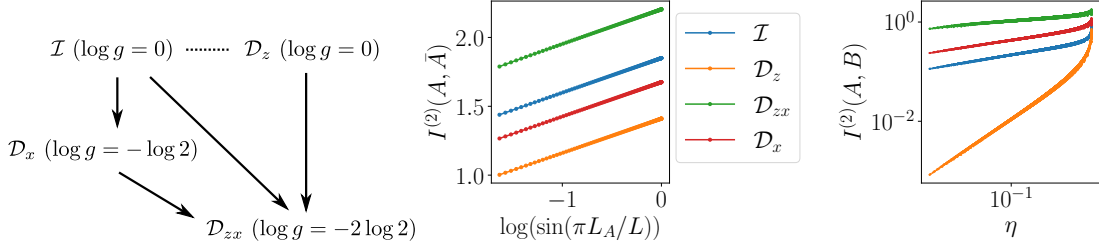


FIG. 3. Fixed-point channels for Ising model and their universal properties. Left: g -function of the four fixed points among dephasing channels and their RG flow. The dashed line indicates that they are connected by marginal deformations and the solid lines indicate direction of the RG flow. Center: $I^{(2)}(A, \bar{A})$ of a single interval at the four fixed points. All four slopes are estimated to be close to $4\Delta_{\mathcal{I}\mathcal{N}}^{(2)} \approx 1/4$. Right: $I^{(2)}(A, B)$ of a two disjoint intervals at the four fixed points. The scaling dimension $\Delta_{\mathcal{O}}^{(2)}$ is close to $1/4, 1, 1/8, 1/4$ for the four fixed points $\mathcal{I}, \mathcal{D}_z, \mathcal{D}_{zx}, \mathcal{D}_x$, respectively.

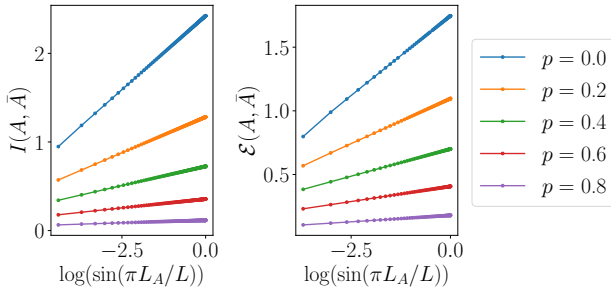


FIG. 4. Mutual information (left) and negativity (right) for free fermion critical state subject to amplitude damping channel of strength p .

Critical Ising model under dephasing noise—As an example, we study the effect of dephasing noise on the ground state of the 1d transverse field Ising model

$$H = - \sum_{i=1}^L \sigma_{x,i} \sigma_{x,i+1} - \sum_{i=1}^L \sigma_{z,i}. \quad (14)$$

For the dephasing noise $\mathcal{D}_{p, \vec{v}}$, we restrict the direction to the XZ plane, i.e., $\vec{v} = (\sin(\pi\tilde{\theta}/2), 0, \cos(\pi\tilde{\theta}/2))$, where $0 \leq \tilde{\theta} \leq 1$. For Renyi index $n = 2$, we find four RG fixed points: (1) identity channel $\mathcal{I} = \mathcal{D}_{0, \vec{v}}$ with $\log g_{\mathcal{I}} = 0$, (2) complete dephasing in Z direction \mathcal{D}_z with $\log g_z = 0$, (3) complete dephasing in X direction \mathcal{D}_x with $\log g_x = -\log 2$ and (4) complete dephasing \mathcal{D}_{zx} at $\tilde{\theta} \approx 0.8$, with

$\log g_{zx} = -2 \log 2$. For complete dephasing, the entropy reduces to the “classical Shannon entropy” of Ref. [44], which considered cases (2) and (3).

We also observe the RG flow between these four fixed points, which manifests the monotonicity of the g -function. Near the \mathcal{D}_z fixed point, we can turn on a small perturbation to $\tilde{\theta}$ and observe the RG flow to the \mathcal{D}_{zx} fixed point. The universal data collapse indicates the critical exponent is $\nu \approx 2.0$. Analogously, near the \mathcal{D}_x fixed point, we can turn on a perturbation to $\tilde{\theta}$ and observe the RG flow to the \mathcal{D}_{zx} fixed point. The universal data collapse shows that $\nu \approx 1.0$. Another example is the RG flow from \mathcal{I} fixed point to complete dephasing \mathcal{D}_{zx} and \mathcal{D}_x by turning on a small p , see appendix. Finally, all dephasing channels $\mathcal{D}_{p,z}$ have the same $\log g = 0$, which suggests that they constitute a continuous family of fixed points connected by marginal deformations. These RG flows are summarized in Fig. 3.

The entropy of a subsystem at the four RG fixed points is shown in Fig. 3. For a single interval, we find that they all satisfy Eq. (11) with the same $\Delta_{\mathcal{I}\mathcal{N}}^{(2)} = 1/16$. For the identity channel, the operator $\phi_{\mathcal{I}\mathcal{N}}^{(2)}$ is the branch-point twist operator, with the scaling dimension $c/8 = 1/16$. The fact that the scaling dimensions coincide for dephasing channel and identity channel was also observed numerically in Ref. [45]. In order to distinguish the channels, we compute the Renyi mutual information

$I^{(n)}(A, B)$ of two disjoint intervals. We see that the scaling dimensions of $\Delta_O^{(2)}$ vary among the four fixed points. These dimensions can be understood analytically in terms of local operators in the two-copied Ising model, see appendix for details.

Finally, for scalable calculation of entanglement negativity, we consider an amplitude damping channel \mathcal{A}_p with variable strength p applied to the 1d critical free Majorana fermion, which is related to the critical Ising model by a Jordan-Wigner transformation (see appendix for details). Again for scalable calculation, we use the generalization of negativity to free fermion systems, in which the partial transpose is replaced by partial time reversal operation [46]. We find that the mutual information and negativity both show logarithmic scaling with coefficient varying continuously with p (see Fig. 4), consistent with a continuous set of fixed points connected by marginal deformations.

Discussion— In this work we have established a notion of RG flow and transitions between quantum channels acting on a critical wavefunction. We have shown that a g -function gives the volume-independent part of the Renyi entropy at the RG fixed points and established its monotonicity under the RG flow. We have demonstrated the RG flow between quantum channels using the example of the transverse field Ising model and dephasing noise, although generalization to other noise models, such as depolarizing noise, is straightforward and also yields interesting phenomena (see appendix for details).

Our notion of RG flow can be naturally applied to measurement-induced quantities of a critical wavefunction, such as those considered in Refs. [23, 24]. Another future direction is to classify the conformal boundary conditions for the fixed-point quantum channels in the CFT and take the replica limit. It is not yet known how this could be done for a generic CFT. Even within minimal models only a few examples have been addressed [47]. Regarding the holographic correspondence between a CFT on the boundary of a spacetime and a gravitational theory in the bulk, it would be interesting to explore the holographic dual of quantum channels acting on the boundary; many recent works have considered coupling the boundary CFT to a bath, and perhaps our formalism could be related to replica wormholes [48–50]. In another direction, while this work only considered one layer of local quantum channels, it may also be interesting to explore the entanglement dynamics of random local channels [51] on quantum critical (and other long-range entangled) states. Finally, we comment that experimental observation of our main results involving Renyi entropy and entanglement negativity can be achieved on quantum computers and simulators using recent techniques of shadow tomography [26, 27].

Acknowledgements— We thank Runze Chi, Paolo Glorioso, Yaodong Li, Yuhan Liu, Peter Lu, Alex May, Xiao-Liang Qi, Guifre Vidal, and Fei Yan for helpful discus-

sions. Y.Z. particularly thanks Ehud Altman, Samuel Garatt and Zack Weinstein for explanation of their work Ref. [24]. We thank Jacob Lin and Weicheng Ye for collaboration on a related project. S.S. and T.H. are supported by Perimeter Institute and NSERC. Research at Perimeter Institute is supported in part by the Government of Canada through the Department of Innovation, Science and Economic Development Canada and by the Province of Ontario through the Ministry of Colleges and Universities. Y. Z. is supported by the Q-FARM fellowship at Stanford University.

Note added: While completing this manuscript, we noticed a related independent work [52].

-
- [1] F. Arute *et al.*, Quantum supremacy using a programmable superconducting processor, *Nature* **574**, 505 (2019), arXiv:1910.11333 [quant-ph].
 - [2] H.-S. Zhong, H. Wang, Y.-H. Deng, M.-C. Chen, L.-C. Peng, Y.-H. Luo, J. Qin, D. Wu, X. Ding, Y. Hu, P. Hu, X.-Y. Yang, W.-J. Zhang, H. Li, Y. Li, X. Jiang, L. Gan, G. Yang, L. You, Z. Wang, L. Li, N.-L. Liu, C.-Y. Lu, and J.-W. Pan, Quantum computational advantage using photons, *Science* **370**, 1460 (2020), <https://www.science.org/doi/pdf/10.1126/science.abe8770>.
 - [3] L. S. Madsen, F. Laudenbach, M. F. Askarani, F. Rortais, T. Vincent, J. F. F. Bulmer, F. M. Miatto, L. Neuhaus, L. G. Helt, M. J. Collins, A. E. Lita, T. Gerrits, S. W. Nam, V. D. Vaidya, M. Menotti, I. Dhand, Z. Vernon, N. Quesada, and J. Lavoie, Quantum computational advantage with a programmable photonic processor, *Nature* **606**, 75 (2022).
 - [4] J. Zhang, G. Pagano, P. W. Hess, A. Kyprianidis, P. Becker, H. Kaplan, A. V. Gorshkov, Z. X. Gong, and C. Monroe, Observation of a many-body dynamical phase transition with a 53-qubit quantum simulator, *Nature* **551**, 601 (2017).
 - [5] H. Bernien, S. Schwartz, A. Keesling, H. Levine, A. Omran, H. Pichler, S. Choi, A. S. Zibrov, M. Endres, M. Greiner, V. Vuletić, and M. D. Lukin, Probing many-body dynamics on a 51-atom quantum simulator, *Nature* **551**, 579 (2017).
 - [6] G. Semeghini, H. Levine, A. Keesling, S. Ebadi, T. T. Wang, D. Bluvstein, R. Verresen, H. Pichler, M. Kalinowski, R. Samajdar, A. Omran, S. Sachdev, A. Vishwanath, M. Greiner, V. Vuletić, and M. D. Lukin, Probing topological spin liquids on a programmable quantum simulator, *Science* **374**, 1242 (2021), <https://www.science.org/doi/pdf/10.1126/science.abi8794>.
 - [7] K. J. Satzinger, Y.-J. Liu, A. Smith, C. Knapp, M. Newman, C. Jones, Z. Chen, C. Quintana, X. Mi, A. Dunsworth, C. Gidney, I. Aleiner, F. Arute, K. Arya, J. Atalaya, R. Babbush, J. C. Bardin, R. Barends, J. Basso, A. Bengtsson, A. Bilmes, M. Broughton, B. B. Buckley, D. A. Buell, B. Burkett, N. Bushnell, B. Chiaro, R. Collins, W. Courtney, S. Demura, A. R. Derk, D. Eppens, C. Erickson, L. Faoro, E. Farhi, A. G. Fowler, B. Foxen, M. Giustina, A. Greene, J. A. Gross, M. P. Harrigan, S. D. Harrington, J. Hilton, S. Hong, T. Huang, W. J. Huggins, L. B. Ioffe, S. V.

- Isakov, E. Jeffrey, Z. Jiang, D. Kafri, K. Kechedzhi, T. Khattar, S. Kim, P. V. Klimov, A. N. Korotkov, F. Kostritsa, D. Landhuis, P. Laptev, A. Locharla, E. Lucero, O. Martin, J. R. McClean, M. McEwen, K. C. Miao, M. Mohseni, S. Montazeri, W. Mruczkiewicz, J. Mutus, O. Naaman, M. Neeley, C. Neill, M. Y. Niu, T. E. O'Brien, A. Opremcak, B. Pató, A. Petukhov, N. C. Rubin, D. Sank, V. Shvarts, D. Strain, M. Szalay, B. Villalonga, T. C. White, Z. Yao, P. Yeh, J. Yoo, A. Zalcman, H. Neven, S. Boixo, A. Megrant, Y. Chen, J. Kelly, V. Smelyanskiy, A. Kitaev, M. Knap, F. Pollmann, and P. Roushan, Realizing topologically ordered states on a quantum processor, *Science* **374**, 1237 (2021), <https://www.science.org/doi/pdf/10.1126/science.abi8378>.
- [8] D. Zhu, S. Johri, N. M. Linke, K. A. Landsman, C. Huerta Alderete, N. H. Nguyen, A. Y. Matsuura, T. H. Hsieh, and C. Monroe, Generation of thermofield double states and critical ground states with a quantum computer, *Proc. Natl. Acad. Sci.* **117**, 25402 (2020).
- [9] B. Skinner, J. Ruhman, and A. Nahum, Measurement-Induced Phase Transitions in the Dynamics of Entanglement, *Physical Review X* **9**, 031009 (2019), arXiv:1808.05953 [cond-mat.stat-mech].
- [10] A. Chan, R. M. Nandkishore, M. Pretko, and G. Smith, Unitary-projective entanglement dynamics, *Phys. Rev. B* **99**, 224307 (2019), arXiv:1808.05949 [cond-mat.stat-mech].
- [11] Y. Li, X. Chen, and M. P. A. Fisher, Quantum Zeno effect and the many-body entanglement transition, *Physical Review B* **98**, 205136 (2018), arXiv:1808.06134 [quant-ph].
- [12] S. Choi, Y. Bao, X.-L. Qi, and E. Altman, Quantum Error Correction in Scrambling Dynamics and Measurement-Induced Phase Transition, *Phys. Rev. Lett.* **125**, 030505 (2020), arXiv:1903.05124 [quant-ph].
- [13] M. J. Gullans and D. A. Huse, Dynamical Purification Phase Transition Induced by Quantum Measurements, *Physical Review X* **10**, 041020 (2020), arXiv:1905.05195 [quant-ph].
- [14] C.-M. Jian, Y.-Z. You, R. Vasseur, and A. W. W. Ludwig, Measurement-induced criticality in random quantum circuits, *Phys. Rev. B* **101**, 104302 (2020), arXiv:1908.08051 [cond-mat.stat-mech].
- [15] Y. Bao, S. Choi, and E. Altman, Theory of the phase transition in random unitary circuits with measurements, *Phys. Rev. B* **101**, 104301 (2020), arXiv:1908.04305 [cond-mat.stat-mech].
- [16] C. de Groot, A. Turzillo, and N. Schuch, Symmetry Protected Topological Order in Open Quantum Systems, *Quantum* **6**, 856 (2022).
- [17] R. Ma and C. Wang, Average symmetry-protected topological phases (2022).
- [18] J. Y. Lee, Y.-Z. You, and C. Xu, Symmetry protected topological phases under decoherence (2022).
- [19] E. Lake, S. Balasubramanian, and S. Choi, Exact quantum algorithms for quantum phase recognition: Renormalization group and error correction (2022).
- [20] R. Fan, Y. Bao, E. Altman, and A. Vishwanath, Diagnostics of mixed-state topological order and breakdown of quantum memory (2023).
- [21] Y. Bao, R. Fan, A. Vishwanath, and E. Altman, Mixed-state topological order and the errorfield double formulation of decoherence-induced transitions (2023).
- [22] M. A. Rajabpour, Entanglement entropy after a partial projective measurement in 1 + 1 dimensional conformal field theories: Exact results, *J. Stat. Mech. Theory Exp.* **6**, 063109 (2016), arXiv:1512.03940 [hep-th].
- [23] C.-J. Lin, W. Ye, Y. Zou, S. Sang, and T. H. Hsieh, Probing sign structure using measurement-induced entanglement (2022).
- [24] S. J. Garratt, Z. Weinstein, and E. Altman, Measurements conspire nonlocally to restructure critical quantum states (2022).
- [25] S. Antonini, G. Bentsen, C. Cao, J. Harper, S.-K. Jian, and B. Swingle, Holographic measurement and bulk teleportation (2022).
- [26] H.-Y. Huang, R. Kueng, and J. Preskill, Predicting many properties of a quantum system from very few measurements, *Nature Physics* **16**, 1050 (2020).
- [27] A. Elben, R. Kueng, H.-Y. R. Huang, R. van Bijnen, C. Kokail, M. Dalmonte, P. Calabrese, B. Kraus, J. Preskill, P. Zoller, and B. Vermersch, Mixed-state entanglement from local randomized measurements, *Physical Review Letters* **125**, 10.1103/physrevlett.125.200501 (2020).
- [28] J. Preskill, *Lecture notes for physics 229: Quantum information and computation* (California Institute of Technology, 1998).
- [29] M. Oshikawa and I. Affleck, Boundary conformal field theory approach to the critical two-dimensional ising model with a defect line, *Nuclear Physics B* **495**, 533 (1997).
- [30] G. Vidal and R. F. Werner, Computable measure of entanglement, *Phys. Rev. A* **65**, 032314 (2002).
- [31] P. Calabrese, J. Cardy, and E. Tonni, Entanglement negativity in quantum field theory, *Physical Review Letters* **109**, 10.1103/physrevlett.109.130502 (2012).
- [32] P. Calabrese and J. Cardy, Time dependence of correlation functions following a quantum quench, *Physical Review Letters* **96**, 10.1103/physrevlett.96.136801 (2006).
- [33] P. Calabrese and J. Cardy, Quantum quenches in extended systems, *Journal of Statistical Mechanics: Theory and Experiment* **2007**, P06008 (2007).
- [34] P. Calabrese and J. Cardy, Quantum quenches in 1 dimensional conformal field theories, *Journal of Statistical Mechanics: Theory and Experiment* **2016**, 064003 (2016).
- [35] J. Cardy, Bulk Renormalization Group Flows and Boundary States in Conformal Field Theories, *SciPost Phys.* **3**, 011 (2017).
- [36] See appendix for more comments on the applicability of conformal boundary conditions to quantum quench problems.
- [37] D. Friedan and A. Konechny, Boundary entropy of one-dimensional quantum systems at low temperature, *Physical Review Letters* **93**, 10.1103/physrevlett.93.030402 (2004).
- [38] H. Casini, I. S. Landea, and G. Torroba, The g-theorem and quantum information theory, *Journal of High Energy Physics* **2016**, 10.1007/jhep10(2016)140 (2016).
- [39] G. Cuomo, Z. Komargodski, and A. Raviv-Moshe, Renormalization group flows on line defects, *Physical Review Letters* **128**, 10.1103/physrevlett.128.021603 (2022).
- [40] I. Affleck and A. W. W. Ludwig, Universal noninteger 'ground state degeneracy' in critical quantum systems, *Phys. Rev. Lett.* **67**, 161 (1991).
- [41] I. Affleck, Boundary condition changing operations in conformal field theory and condensed matter physics, Nu-

- clear Physics B - Proceedings Supplements **58**, 35 (1997), proceedings of the European Research Conference in the Memory of Claude Itzykson.
- [42] Y. Li, X. Chen, A. W. W. Ludwig, and M. P. A. Fisher, Conformal invariance and quantum nonlocality in critical hybrid circuits, *Physical Review B* **104**, 10.1103/physrevb.104.104305 (2021).
- [43] P. Calabrese, C. Hagendorf, and P. L. Doussal, Time evolution of one-dimensional gapless models from a domain wall initial state: stochastic loewner evolution continued?, *Journal of Statistical Mechanics: Theory and Experiment* **2008**, P07013 (2008).
- [44] J.-M. Stéphan, S. Furukawa, G. Misguich, and V. Pasquier, Shannon and entanglement entropies of one- and two-dimensional critical wave functions, *Physical Review B* **80**, 10.1103/physrevb.80.184421 (2009).
- [45] F. C. Alcaraz and M. A. Rajabpour, Universal behavior of the Shannon mutual information of critical quantum chains, *Physical Review Letters* **111**, 10.1103/physrevlett.111.017201 (2013).
- [46] H. Shapourian, K. Shiozaki, and S. Ryu, Partial time-reversal transformation and entanglement negativity in fermionic systems, *Physical Review B* **95**, 10.1103/physrevb.95.165101 (2017).
- [47] T. Quella, I. Runkel, and G. M. Watts, Reflection and transmission for conformal defects, *Journal of High Energy Physics* **2007**, 095 (2007).
- [48] A. Almheiri, N. Engelhardt, D. Marolf, and H. Maxfield, The entropy of bulk quantum fields and the entanglement wedge of an evaporating black hole, *Journal of High Energy Physics* **2019**, 63 (2019).
- [49] G. Penington, S. H. Shenker, D. Stanford, and Z. Yang, Replica wormholes and the black hole interior, *Journal of High Energy Physics* **2022**, 205 (2022).
- [50] A. Almheiri, T. Hartman, J. Maldacena, E. Shaghoulian, and A. Tajdini, Replica wormholes and the entropy of Hawking radiation, *Journal of High Energy Physics* **2020**, 13 (2020).
- [51] Z. Li, S. Sang, and T. H. Hsieh, Entanglement dynamics of random quantum channels (2022).
- [52] J. Y. Lee, C.-M. Jian, and C. Xu, Quantum criticality under decoherence or weak measurement (2023).
- [53] Y. Liu, R. Sohal, J. Kudler-Flam, and S. Ryu, Multipartitioning topological phases by vertex states and quantum entanglement, *Physical Review B* **105**, 10.1103/physrevb.105.115107 (2022).
- [54] Y. Zou, A. Milsted, and G. Vidal, Conformal fields and operator product expansion in critical quantum spin chains, *Physical Review Letters* **124**, 10.1103/physrevlett.124.040604 (2020).

ISING MODEL WITH FINITE DEPHASING AND DEPOLARIZING NOISE

In this appendix, we consider channels beyond fixed point channels. In particular, we consider finite dephasing and depolarizing channels and their flow to the fixed points. The dephasing channel is defined by

$$\mathcal{D}_{p,\vec{v}}(\rho) = \left(1 - \frac{p}{2}\right)\rho + \frac{p}{2}\sigma_{\vec{v}}\rho\sigma_{\vec{v}}. \quad (15)$$

We fix \vec{v} and continuously change p away from the fixed point $p_c = 0$. We compute the g -function for the second Renyi entropy. As shown in Fig. 5, the g -function has a universal form

$$g^{(2)}(p, L) = g^{(2)}(pL^{1/\nu}), \quad (16)$$

where ν depends on the direction \vec{v} , indicating flow from \mathcal{I} to different IR fixed points. For flow to \mathcal{D}_{zx} , we have $1/\nu \approx 0.8$, and for flow to \mathcal{D}_x , we have $1/\nu \approx 0.7$.

Next, we consider a different class of noise channels, the depolarizing noise, whose action on a single qubit is

$$\Delta_p(\rho) = (1 - p)\rho + \frac{p}{2}I. \quad (17)$$

At $p = 0$, the channel is the \mathcal{I} channel, which is a fixed point with $\log g = 0$. At $p = 1$, the channel turns any state into a maximally mixed state, thus it is also a fixed point with $\log g = 0$. We denote the latter fixed point by Δ_1 . Surprisingly, we find another fixed point at $p \approx 0.7$, which has $\log g^{(2)} \approx -\log 2$, see Fig. 6. We denote this fixed point as Δ . By turning on a small perturbation to p at either the \mathcal{I} ($p = 0$) or Δ_1 ($p = 1$) fixed point, the channel flows to the new fixed point Δ . The data collapse shows that the critical exponent is $1/\nu \approx 0.7$ and $1/\nu \approx 0.9$, respectively.

We suspect that the finite-depolarization fixed point Δ coincides with the complete dephasing \mathcal{D}_x fixed point for the ground state of transverse-field Ising model. They both have $\log g^{(2)} \approx -\log 2$, and the scaling dimension of the boundary condition changing operator $\phi_{\mathcal{IN}}^{(2)}$ are both approximately $1/16$. Furthermore, the RG flow from \mathcal{I} to both fixed point has the same critical exponent $1/\nu \approx 0.7$, and the subsystem entropy both shows a transient scaling with close transient scaling dimensions (see the section below). We leave it as future work to determine whether Δ is the same fixed point as \mathcal{D}_x from the boundary CFT perspective.

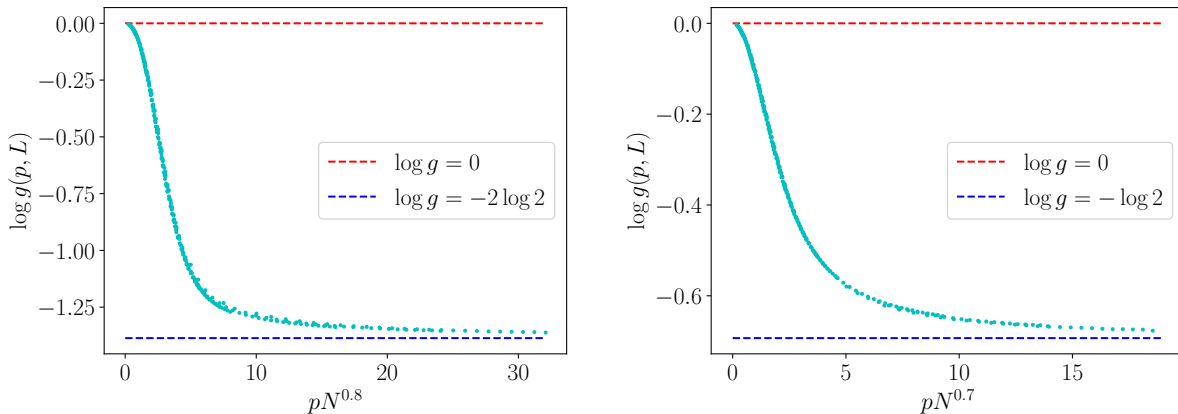


FIG. 5. g -function of dephasing channel $\mathcal{D}_{p,\vec{v}}$ where $0 \leq p \leq 0.3$. Left: $\tilde{\theta} = 0.6$ in the ZX direction, indicating RG flow from \mathcal{I} to \mathcal{D}_{zx} . Right: $\tilde{\theta} = 1$, indicating RG flow from \mathcal{I} to \mathcal{D}_x .

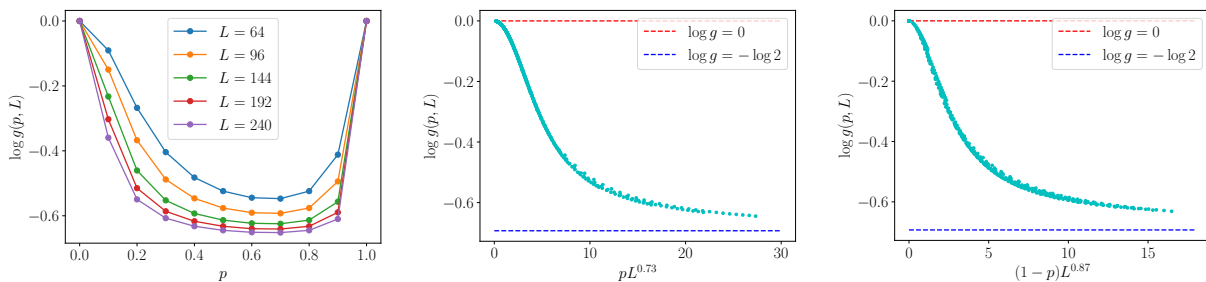


FIG. 6. g -function of depolarization channel Δ_p . Left: $g(p, L)$ for different L . Center: Data collapse for $0 \leq p \leq 0.2$, indicating RG flow from \mathcal{I} to Δ . Right: Data collapse for $0.85 \leq p \leq 1$, indicating RG flow from Δ_1 to Δ .

TRANSIENT BEHAVIOR OF SUBSYSTEM ENTROPY

We have shown that at the fixed points the subsystem entropy satisfies a simple formula

$$I^{(n)}(A, \bar{A}) = \frac{4\Delta_{\mathcal{I}\mathcal{N}}^{(n)}}{n-1} \log \left(\frac{L}{\pi} \sin \left(\frac{\pi L_A}{L} \right) \right) + O(1). \quad (18)$$

Away from the fixed points, the formula is expected to hold in the limit of $L_A \rightarrow \infty$, $L \rightarrow \infty$ while keeping L_A/L a $O(1)$ constant. However, when the channel is in the middle of a RG flow between fixed points, interesting transient behaviors occur at finite sizes. We show numerically that Eq. (18) still approximately holds, but with scaling dimensions $\Delta_{\mathcal{I}\mathcal{N}}^{(n)}$ drifting with the system sizes. We study two examples of RG flow in more detail below.

RG flow from \mathcal{D}_x to \mathcal{D}_{zx}

As a first example, we study the complete dephasing channel $\mathcal{D}_{p,\vec{v}}$ with $p = 1$ and $\vec{v} = (\sin(\pi\tilde{\theta}/2), 0, \cos(\pi\tilde{\theta}/2))$ acting on the ground state of the critical Ising model. We choose $\tilde{\theta}$ close to 1 to observe a RG flow from the UV fixed point \mathcal{D}_x to IR fixed point \mathcal{D}_{zx} . We plot the Renyi mutual information $I^{(2)}(A, \bar{A})$ in Fig. 7.

We see that at large L_A and L the subsystem entropy agrees with the IR fixed point with $4\Delta_{\mathcal{I}\mathcal{N}}^{(2)} = 1/4$. At smaller sizes we see a transient scaling with $4\Delta_{\mathcal{I}\mathcal{N}}^{(2)} = 1/2$. The crossover between the two scaling can be tuned by varying $\tilde{\theta}$. The length scales where we observe the transient scaling become broader if we tune $\tilde{\theta}$ closer to the UV fixed point $\tilde{\theta} = 1$, as the RG flow becomes longer. We conjecture that the operator with $4\Delta_{\mathcal{I}\mathcal{N}}^{(2)} = 1/2$ is the subleading boundary

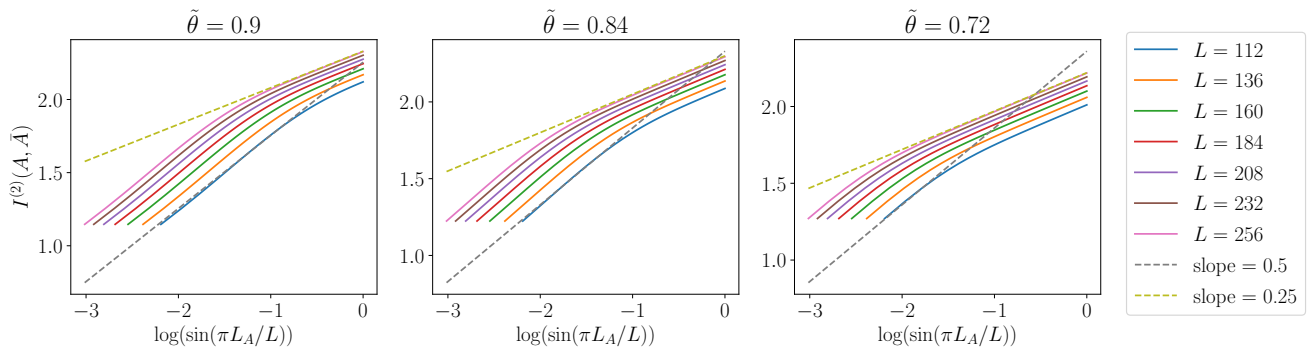


FIG. 7. Renyi mutual information $I^{(2)}(A, \bar{A})$ for the complete dephasing channel acting on the ground state of Ising model.

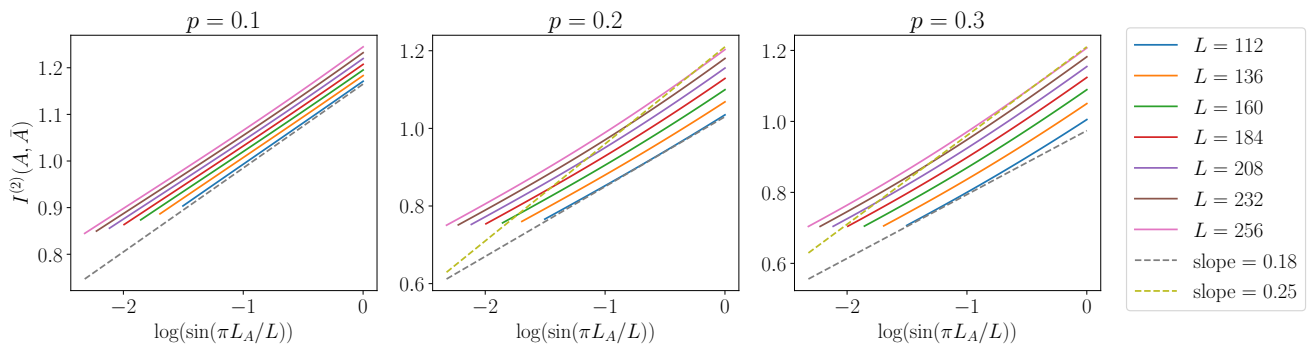


FIG. 8. Renyi mutual information $I^{(2)}(A, \bar{A})$ for the depolarization channel acting on the ground state of Ising model.

condition changing operator from $|B_{\mathcal{I}}\rangle\rangle$ to $|B_{\mathcal{N}}\rangle\rangle$ at the IR fixed point, where $\mathcal{N} = \mathcal{D}_{zx}$. We leave it for future work to identify these operators in the replicated CFT.

RG flow from \mathcal{I} to Δ

Next, we consider the RG flow from identity channel \mathcal{I} to finite depolarization Δ fixed point. We consider depolarization channel Δ_p with $p = 0.1, 0.2, 0.3$ and plot the Renyi mutual information $I(A, \bar{A})$ in Fig. 8. Again, we see that there is a transient behavior at small sizes near the UV fixed point. At $p = 0.1$, Eq. (18) holds with $4\Delta_{\mathcal{I}\mathcal{N}}^{(2)} \approx 0.18$ for all sizes $L \leq 256$. At larger p and larger sizes, the IR scaling with $4\Delta_{\mathcal{I}\mathcal{N}}^{(2)} \approx 1/4$ starts to emerge. The appearance of drifting scaling dimension at small sizes is similar to the previous example.

We note that the same transient behavior is observed for finite dephasing channel $\mathcal{D}_{p,x}$. At small p and small system sizes, e.g., $p = 0.1$ and $L \leq 256$, we also observe that Eq. (18) holds with $4\Delta_{\mathcal{I}\mathcal{N}}^{(2)} \approx 0.18$. This provide additional evidence that Δ and \mathcal{D}_x may be the same fixed point, although a more detailed field-theoretic computation must be done in order to show it.

FREE FERMION WITH AMPLITUDE DAMPING NOISE

In this appendix, we provide additional details on the free fermion numerical results in the main text. We consider the free Majorana fermion with Neveu-Schwarz boundary condition

$$H = -2i \sum_{j=1}^{2L} \psi_j \psi_{j+1}, \quad (19)$$

where ψ_j is the Majorana operator that satisfies $\{\psi_j, \psi_l\} = \delta_{jl}$, and $\psi_{2N+1} = -\psi_1$. The Hamiltonian is equivalent to the transverse field Ising model under the Jordan-Wigner transformation. Yet, a local channel in the spin representation may not be a local channel in the fermion representation.

Here we use the covariance matrix technique to simulate the amplitude damping channel, which is a Gaussian channel. The covariance matrix, defined by

$$M_{jl} = -i\text{Tr}((\psi_j\psi_l - \delta_{jl})\rho), \quad (20)$$

fully characterizes a Gaussian state ρ . One may introduce complex fermion operators $c_j = (\psi_{2j} - i\psi_{2j+1})/\sqrt{2}$, $c_j^\dagger = (\psi_{2j} + i\psi_{2j+1})/\sqrt{2}$ and the number operator $c_j^\dagger c_j$. The amplitude damping channel \mathcal{A}_p for a single fermion can be realized by

$$\mathcal{A}_p(\rho_S) = \text{Tr}_A[U_{p,SA}(\rho_S \otimes |0\rangle_A \langle 0|)U_{p,SA}^\dagger], \quad (21)$$

where $|0\rangle_A$ is the ground state of the number operator $c_A^\dagger c_A$ of the ancilla, and

$$U_{p,SA} = e^{\theta(c_S^\dagger c_A - c_A^\dagger c_S)}, \quad p = \sin^2 \theta. \quad (22)$$

Such representation makes it clear that the amplitude damping channel is a Gaussian channel. The channel on the total system is a product of single-fermion channels, $\mathcal{N}_p = \otimes_j \mathcal{A}_{p,j}$. The covariance matrix M_p of the decohered state $\mathcal{N}_p(\rho)$ is

$$M_p = (1-p)M + pM^{(0)}, \quad (23)$$

where M is the covariance matrix of ρ and $M^{(0)}$ is the covariance matrix of $|0\rangle^{\otimes L}$ with nonzero entries $M_{2i-1,2i}^{(0)} = -M_{2i,2i-1}^{(0)} = 1$. Using the covariance matrix, one may compute all the Renyi mutual information $I^{(n)}(A, B)$ and Renyi negativity $\mathcal{E}^{(n)}(A, B)$ of any two subsystems. One can directly take the replica limit to obtain the Von-Neumann mutual information $I(A, B)$ and the logarithmic negativity $\mathcal{E}(A, B)$ of the decohered state. We note that here the negativity is defined through partial time reversal rather than partial transpose, following the computation of Refs. [46, 53].

As shown in the main text, we find that the amplitude damping channel forms a continuous set of conformal fixed points with $\log g^{(n)} = 0$ for any n . The scaling dimension of the boundary condition changing operator $\phi_{\mathcal{I}\mathcal{N}}^{(n)}$ also continuously changes with the damping strength p , as is evident by the (Renyi) mutual information $I^{(n)}(A, \bar{A})$. Likewise, the (Renyi) negativity $\mathcal{E}^{(n)}(A, \bar{A})$ shows a similar logarithmic form with continuously changing coefficients.

ANALYTICAL TREATMENT OF RENEYI MUTUAL INFORMATION

Here we present analytical result of Renyi mutual information $I^{(n)}(A : B)$, where A and B are of $O(1)$ size. We show that $I^{(n)}(A : B)$ decays as a power law of the distance and the power is determined by the quantum channel. For the case of dephasing channel and $|A|, |B| = 1$, we further take the replica limit $n \rightarrow 1$ and consider the Von-Neumann mutual information. Our results provide a concrete example where any Renyi mutual information with $n > 1$ is not monotonic under local quantum channels, in sharp contrast with the Von-Neumann mutual information.

Renyi mutual information of two sites

Let $|A| = |B| = 1$, then

$$I^{(n)}(A : B) = \frac{1}{n-1} \log \frac{\langle \mathcal{N}^*(\tau_{n,A}) \mathcal{N}^*(\tau_{n,B}) \rangle}{\langle \mathcal{N}^*(\tau_{n,A}) \rangle \langle \mathcal{N}^*(\tau_{n,B}) \rangle}, \quad (24)$$

where the expectation value is taken on the ground state of n -copied CFT. Let the distance of A and B be l and let

$$d = \frac{l}{\pi} \sin \frac{\pi l}{L} \quad (25)$$

be the chord distance. We can expand the lattice operator $B_{\mathcal{N}}^{(n)} = \mathcal{N}^*(\tau_n)$ into a sum of CFT operators in n -copied CFT,

$$B_{\mathcal{N}}^{(n)} = a_0 I + a_1 O^{(n)} + \dots, \quad (26)$$

where the \dots represents operators with higher scaling dimensions. The correlation function $\langle O^{(n)}(x)O^{(n)}(y) \rangle \sim d^{-2\Delta_O^{(n)}}$, thus

$$I^{(n)}(A : B) \sim d^{-2\Delta_O^{(n)}}. \quad (27)$$

Renyi index $n = 2$

For complete dephasing, we compute the lattice operator and find their CFT counterpart using the dictionary in Ref. [54]. Below we list results for various choices of \vec{v} in the dephasing channel. For the fixed points $\mathcal{D}_z, \mathcal{D}_x, \mathcal{D}_{zx}$, we find that the leading CFT operator to $O^{(2)}$ is $\varepsilon \otimes I + I \otimes \varepsilon, \sigma \otimes \sigma$ and $\sigma \otimes I + I \otimes \sigma$, with scaling dimension $1, 1/4, 1/8$ respectively. This agrees with the numerical result shown in the main text, $I^{(2)}(A, B) \sim \eta \Delta_O^{(2)}$. However, we note an important difference: in the main text we consider $|A|$ and $|B|$ to be much larger than the lattice spacing rather than $|A| = |B| = 1$. It is not a priori the case that the scaling operators $O^{(n)}$ are the same for the two cases. Yet for the dephasing fixed points we observe that they coincide.

We also note that the exponent $1/8$ for \mathcal{D}_{zx} is smaller than that of the identity channel, meaning that the channel increases the Renyi mutual information. As we show shortly, this happens for all Renyi indices $n > 1$, but ceases to hold at $n = 1$.

Dephasing direction \vec{v}	$O^{(2)}$ (leading)	CFT operator	$\Delta_O^{(2)}$
\vec{x}	$X \otimes X$	$\sigma \otimes \sigma$	1/4
\vec{y}	$Y \otimes Y$	$\partial_\tau \sigma \otimes \partial_\tau \sigma$	9/4
\vec{z}	$Z \otimes Z$	$\varepsilon \otimes I + I \otimes \varepsilon$	1
Generic $(v_x, v_y, 0)$	$X \otimes X$	$\sigma \otimes \sigma$	1/4
Generic $(v_x, 0, v_z)$	$X \otimes Z + Z \otimes X$	$\sigma \otimes I + I \otimes \sigma$	1/8
Generic $(0, v_y, v_z)$	$Z \otimes Z$	$\varepsilon \otimes I + I \otimes \varepsilon$	1
Generic (v_x, v_y, v_z)	$X \otimes Z + Z \otimes X$	$\sigma \otimes I + I \otimes \sigma$	1/8

TABLE I. Scaling dimension of $O^{(2)}$ under complete dephasing ($p = 1$) in different directions. (“Generic” means all components are nonzero.)

Higher Renyi index

For general replica number $n \geq 2$, we first consider the \vec{z} direction dephasing,

$$B_{\mathcal{N}}^{(n)} := \mathcal{D}_{p=1, \vec{z}}^{*\otimes n}(\tau_n) = \sum_{i=0}^1 |i^{\otimes n}\rangle \langle i^{\otimes n}| \quad (28)$$

In Pauli basis, this is

$$\mathcal{D}_{p=1, \vec{z}}^{*\otimes n}(\tau_n) = \frac{1}{2^{n-1}} \sum_{s \in S_{\vec{z}}} s, \quad (29)$$

where $S_{\vec{z}}$ is the stabilizer group consisting of even number of product of Pauli Z 's. Note that this expression also holds if we change z to any \vec{v} and correspondingly the stabilizer group $S_{\vec{z}}$ to $S_{\vec{v}}$ (which is isomorphic to $S_{\vec{z}}$ by changing Z to $\vec{v} \cdot \vec{\sigma}$). Now we consider the correlation function of this operator on A and B . Taking into account that the correlation function of a single Pauli string factorizes into product of correlation functions of one replica, we obtain

$$\langle \psi^{\otimes n} | B_{\mathcal{N}}^{(n)}(x) B_{\mathcal{N}}^{(n)}(y) | \psi^{\otimes n} \rangle = ((1+x)^2 + C)^n + ((1-x)^2 + C)^n + 2(1-x^2 - C)^n \quad (30)$$

$$\langle \psi^{\otimes n} | B_{\mathcal{N}}^{(n)}(x) | \psi^{\otimes n} \rangle \langle \psi^{\otimes n} | B_{\mathcal{N}}^{(n)}(y) | \psi^{\otimes n} \rangle = (1+x)^{2n} + (1-x)^{2n} + 2(1-x^2)^n \quad (31)$$

where $x = \langle \sigma_{\vec{v}} \rangle$, $C = \langle \sigma_{\vec{v}}(x) \sigma_{\vec{v}}(y) \rangle_c$ is the connected correlation function of the ground state, and $\sigma_{\vec{v}} \equiv \vec{v} \cdot \vec{\sigma}$. The Renyi mutual information is given by

$$I^{(n)}(A, B) = \frac{1}{n-1} \log \frac{\langle \psi^{\otimes n} | B_{\mathcal{N}}^{(n)}(x) B_{\mathcal{N}}^{(n)}(y) | \psi^{\otimes n} \rangle}{\langle \psi^{\otimes n} | B_{\mathcal{N}}^{(n)}(x) | \psi^{\otimes n} \rangle \langle \psi^{\otimes n} | B_{\mathcal{N}}^{(n)}(y) | \psi^{\otimes n} \rangle}. \quad (32)$$

In the case of $n = 2$, this reduces to

$$I^{(2)}(A, B) = \log \left(1 + \frac{x^2 C + C^2}{(1+x^2)^2} \right) \quad (33)$$

In the limit where $C \ll 1$, we obtain

$$I^{(2)}(A, B) = \frac{x^2 C + C^2}{(1+x^2)^2} \quad (C \ll 1) \quad (34)$$

This is in agreement with our previous subsections. If $x = 0$, that is, if the dephasing direction has $v_x = 0$, then $I^{(2)}$ is proportional to the square of correlation function. However, if $x \neq 0$, then $I^{(2)}$ gets promoted to linear in the correlation function. This means that dephasing can actually increase the second Renyi mutual information (e.g., for \mathcal{D}_{zx}). More generally, if $n \geq 2$, we have

$$I^{(n)}(A, B) = \frac{1}{n-1} \log \left(1 + \frac{n((1+x)^{n-1} - (1-x)^{n-1})^2 C + O(C^2)}{((1+x)^n + (1-x)^n)^2} \right), \quad (35)$$

which reduces to

$$I^{(n)}(A, B) = \frac{n}{n-1} \frac{((1+x)^{n-1} - (1-x)^{n-1})^2}{((1+x)^n + (1-x)^n)^2} C + O(C^2), \quad (n \geq 2, C \ll 1) \quad (36)$$

Thus, for all Renyi mutual information $I^{(n)}(A, B)$ with $n > 1$, it can be promoted to linear in correlation function by acting with a dephasing channel $\mathcal{D}_{p=1, \vec{v}}$ if $C := \langle \sigma_{\vec{v}} \rangle \neq 0$.

Replica limit $n \rightarrow 1$

One important point is that the Von Neumann mutual information cannot increase under noise channels. To see this, we use the data processing inequality in quantum information theory

$$S(\mathcal{N}(\rho) | \mathcal{N}(\sigma)) \leq S(\rho | \sigma) \quad (37)$$

Using the fact that $I(A, B) = S(\rho_{AB} | \rho_A \otimes \rho_B)$ and the fact that $\mathcal{N} = \mathcal{N}_A \otimes \mathcal{N}_B$, we obtain

$$I(A, B)_{\mathcal{N}(\rho)} \leq I(A, B)_{\rho}. \quad (38)$$

The data processing inequality does not apply to the Renyi entropies, so the Renyi mutual information is not monotonic under product channels.

The information-theoretic argument dictates that the Von Neumann mutual information after applying the noise channel should be at least quadratic in the original correlation functions. In order to see this, we take the replica limit $n \rightarrow 1$. The result is

$$I(A, B) = \left(H \left(\frac{(1+x)^2 + C}{4} \right) + H \left(\frac{(1-x)^2 + C}{4} \right) + 2H \left(\frac{1-x^2 - C}{4} \right) \right) - (C \leftarrow 0) \quad (39)$$

where $H(x) = x \log x$. Note that the approximation with $C \ll 1$ must come *after* taking the replica limit. Using the Taylor expansion around $C = 0$, and the derivatives $H'(x) = 1 + \log x$, $H''(x) = 1/x$, we obtain

$$I(A, B) = \frac{C^2}{2(1-x^2)^2} \quad (C \ll 1). \quad (40)$$

Note that the linear term in C exactly cancels. Thus we expect that

$$I(A, B) = O(d^{-4\Delta_{\vec{v}, \vec{\sigma}}}) \quad (41)$$

under complete dephasing. See the table below for a list of scaling dimensions for different dephasing channels. We no longer observe an increase in the Von-Neumann mutual information, as required by the data processing inequality.

Dephasing direction \vec{v}	$\vec{v} \cdot \vec{\sigma}$ (leading)	CFT operator	$4\Delta_{\vec{v} \cdot \vec{\sigma}}$
\vec{x}	X	σ	1/2
\vec{y}	Y	$\partial_\tau \sigma$	9/2
\vec{z}	Z	ε	4
Generic $(v_x, v_y, 0)$	X	σ	1/2
Generic $(v_x, 0, v_z)$	X	σ	1/2
Generic $(0, v_y, v_z)$	Z	ε	4
Generic (v_x, v_y, v_z)	X	σ	1/2

TABLE II. Mutual information scaling under complete dephasing ($p = 1$) in different directions.

APPLICABILITY OF CONFORMAL BOUNDARY CONDITIONS

In a global quantum quench problem to a critical Hamiltonian, not all short-range entangled initial state flows to a conformal boundary state. Yet, it has been argued by Cardy [35] that the ground state of the CFT Hamiltonian perturbed by a relevant deformation flows to a Cardy state, a conformal boundary state subject to physical constraints.

In this appendix, we show that the state $|B_{\mathcal{N}}\rangle\rangle$ for a dephasing channel considered in the main text can be associated with such relevant deformations to the $2n$ -copied Ising model. Thus, if the above Cardy's conjecture holds, we can argue that $|B_{\mathcal{N}}\rangle\rangle$ in the main text all flows to conformal boundary states. We also provide an example of \mathcal{N} such that the argument fails and such that $|B_{\mathcal{N}}\rangle\rangle$ does not flow to a conformal boundary state. We will stay within replica index $n = 2$ in this appendix.

To start with, we consider the case where $\mathcal{N} = \mathcal{D}_{p=1,x}$. In this case the operator

$$B_{\mathcal{N}}^{(2)} := \mathcal{N}^{*\otimes 2}(\tau_2) = \frac{1}{2}(I + X \otimes X) \quad (42)$$

Under the folding, the operator becomes a state in 4 replicas, which is

$$|B_{\mathcal{N}}^{(2)}\rangle\rangle = \frac{1}{2}(|+++\rangle + |--\rangle), \quad (43)$$

where $|+\rangle$ or $|-\rangle$ are the eigenstates of X in one replica. One parent Hamiltonian of $|B_{\mathcal{N}}^{(2)}\rangle\rangle$ is

$$H_{int,\mathcal{N}}^{(2)} = X \otimes X \otimes I \otimes I + I \otimes X \otimes X \otimes I + I \otimes I \otimes X \otimes X. \quad (44)$$

The state $|B_{\mathcal{N}}^{(2)}\rangle\rangle$ is its unique ground state upon fixing the total parity. Note that this Hamiltonian is defined on *one* lattice site across the four replicas. Now we consider the replicated CFT Hamiltonian

$$H_C^{(2)} = H_C \otimes I \otimes I \otimes I + I \otimes H_C \otimes I \otimes I + I \otimes I \otimes H_C \otimes I + I \otimes I \otimes I \otimes H_C, \quad (45)$$

where H_C is the Hamiltonian for one copy of critical Ising model. Now we consider the perturbation of $H_C^{(2)}$ by the parent Hamiltonian,

$$H^{(2)} = H_C^{(2)} + \lambda \sum_{j=1}^L H_{int,\mathcal{N},j}^{(2)} \quad (46)$$

The interaction term $H_{int,\mathcal{N}}^{(2)}$ is a *relevant* deformation since its scaling dimension is $2\Delta_\sigma = 1/4 < 2$. At long wavelengths, the coupling λ flows to infinity, and the ground state of $H^{(2)}$ is qualitatively the same as the ground state of $H_{int,\mathcal{N}}^{(2)}$, which is $|B_{\mathcal{N}}^{(2)}\rangle\rangle$. Thus, if the aforementioned Cardy's conjecture holds, then $|B_{\mathcal{N}}^{(2)}\rangle\rangle$ can be described by a conformal boundary state.

In order to generalize the argument to other dephasing channels, we just have to replace X in the parent Hamiltonian $H_{int,\mathcal{N}}^{(2)}$ by $\sigma_{\vec{v}} = \vec{v} \cdot \vec{\sigma}$. If \vec{v} is in the XZ plane, then all terms in the parent Hamiltonian are relevant (they are either $\sigma \otimes \sigma$, $\sigma \otimes I$ or $\sigma \otimes \varepsilon$), and the argument above goes through. We note in passing that for all Renyi index $n \geq 2$ the argument also holds. However, if \vec{v} is in the YZ plane, then not all terms are relevant. For example, the term

$Y \otimes Y \otimes I \otimes I$ has a scaling dimension $2\Delta_{\partial\sigma} = 9/4 > 2$. Then it is no longer guaranteed that the boundary state $|B_{\mathcal{N}}^{(2)}\rangle\rangle$ flows to a conformal boundary condition.

The applicability of conformal boundary condition is crucial to all the main results. The main results could fail, if the boundary state $B_{\mathcal{N}}^{(n)}$ does not flow to a conformal boundary state. Indeed, if we choose $\vec{v} = (0, \sin \theta, \cos \theta)$ in the YZ plane, then we observe that the g -function is monotonically increasing rather than decreasing for a range of θ , e.g., $0 < \theta < \pi/4$. Yet, the g -function still appears to converge at large L , indicating scale invariance. These boundary conditions may be examples of scale invariant but not conformal boundary conditions in the replicated CFT. We leave it as future work to explore these boundary conditions.

NUMERICAL TECHNIQUES

In this appendix, we describe matrix product state techniques to evaluate $S_A^{(n)}(\mathcal{N}(|\psi\rangle\langle\psi|))$. For the sake of presentation, all the tensor diagrams were drawn for the special case that $n = 2$, $L = 4$ and $A = \{1, 2\}$, however the generalization to generic cases is straightforward.

By performing density matrix renormalization group (DMRG) simulation, one is able to obtain the matrix product state (MPS) representation of the critical ground state $|\psi\rangle$ of interest:

$$|\psi\rangle = \begin{array}{c} | \\ \square \\ | \end{array} - \begin{array}{c} | \\ \square \\ | \end{array} - \begin{array}{c} | \\ \square \\ | \end{array} - \begin{array}{c} | \\ \square \\ | \end{array} \quad (47)$$

Accordingly, the partition function $Z_A^{(n)}$ can be diagrammatically represented as:

$$Z_{A=\{1,2\}}^{(n=2)} = \begin{array}{c} \square \\ \square \\ \square \\ \square \end{array} \begin{array}{c} \square \\ \square \\ \square \\ \square \end{array} \begin{array}{c} \square \\ \square \\ \square \\ \square \end{array} \begin{array}{c} \square \\ \square \\ \square \\ \square \end{array} \quad (48)$$

By contracting from left to right, the diagram can be contracted with a time complexity $O(L\chi^{2n+1})$, where χ is the maximum bond dimension of the MPS. Using the above techniques, we can evaluate $Z^{(2)}$ for χ up to 100 and L up to 256.

By replacing I with τ_n^{-1} , the same technique can also be used for evaluating Renyi entanglement negativity.